Journal of Applied and Computational Mechanics, Vol. 2, No. 4, (2016), 208-221
DOI: 10.22055/JACM.2016.12527

Journal of
Applied and Computational Mechanics

Nonlinear Vibration Analysis of Single-Walled Carbon Nanotube Conveying Fluid in Slip Boundary Conditions Using Variational Iterative Method

Gbeminiyi M. Sobamowo

Department of Mechanical Engineering, University of Lagos, Akoka, Lagos, Nigeria.

Received November 05 2016; revised December 12 2016; accepted for publication December 20 2016.
Corresponding author: Gbeminiyi M. Sobamowo, mikegbeminiyiprof@yahoo.com

Abstract

In this paper, nonlinear dynamic behaviour of the carbon nanotube conveying fluid in slip boundary conditions is studied using the variation iteration method. The developed solutions are used to investigate the effects of various parameters on the nonlinear vibration of the nanotube. The results indicate that an increase in the slip parameter leads to a decrease in the frequency of vibration and the critical velocity, while the natural frequency and the critical fluid velocity increase as the stretching effect increases. Also, as the nonlocal parameter increases, the natural frequency and the critical velocity decreases. The analytical solutions help to have better insights and understand the relationship between the physical quantities of the problem.

Keywords: Non-linear vibration; Slip boundary condition; Fluid-conveying nanotube; Variational iteration method.

1. Introduction

Following the discovery of the nanotube by Iijima [1], there have been rapid developments of nanotechnology due to the unique mechanical, thermal, chemical, electrical, electrochemical, and electronic properties of the carbon nanotube (CNT). As one of the various applications of CNT, it has been used for conveying fluid, and the study of the effects and conditions of the moving fluid on the overall mechanical behaviour of CNTs has aroused significant research interests. Consequently, the dynamic analysis of flow-induced vibration of CNT has led to a large number of studies in the literature in recent years [2-9]. Modeling the dynamic behaviours of the structures under the influence of some thermo-fluidic or thermo-mechanical parameters often results in nonlinear equations; thus, it is difficult to find the exact analytical solutions. In some cases, where spatio-temporal decomposition procedures are carried out, the resulting nonlinear equation for the temporal part comes in the form of the Duffing equation. The application of analytical methods such as the Exp-function method, He's Exp-function method, the improved F-expansion method, the Lindstedt-Poincare techniques, and the quotient trigonometric function expansion method to the nonlinear equation presents analytical solutions, either in implicit or explicit form, which often involve complex mathematical analysis leading to an analytic expression which involve a large number of terms. Furthermore, the methods are time-consuming tasks which require high skills in mathematics. Also, they do not provide general analytical solutions since the solutions are often accompanied with conditional statements which make them limited in use because many conditions accompanied with the exact solutions do not meet up with the practical applications. In practice, the analytical solutions with large number of terms and conditional statements are not convenient for use by designers and engineers [10]. Consequently, recourse has always been made to the numerical methods or the approximate analytical methods in solving the problems. However, the classical way for finding an analytical solution is still very important since it serves as an accurate benchmark for the numerical solutions. Moreover, the experimental data are useful to access the mathematical models but are never sufficient to verify the numerical solutions of the established mathematical models. The comparison between the numerical calculations and the experimental data often fails to reveal the compensation of the modelling deficiencies through the computational errors or the unconscious approximations in establishing applicable numerical schemes. Additionally, the analytical solutions for specified

problems are essential for the development of efficient applicable numerical simulation tools. Inevitably, exact analytical expressions are required to show the direct relationship between the models' parameters. When such analytical solutions are available, they provide good insights into the significance of various system parameters affecting the phenomena, as they give continuous physical insights than pure numerical or computation methods. Furthermore, most of the analytical approximations and the purely numerical methods that were applied to the nonlinear problems are computationally intensive in the literature. An analytical expression is more convenient for the engineering calculations compared with the experimental or numerical studies, and it is obviously a starting point for a better understanding of the relationship between physical quantities. It is convenient for the parametric studies accounting for the physical quantities of the problem. The analytical expression appears more appealing than the numerical solution as it helps to reduce the computation costs, simulations, and tasks in the analysis of the real life problems. Therefore, an exact analytical solution is required for the problem. Different approximate analytical methods such as the Perturbation method (regular or singular perturbation method), the homotopy perturbation method (HPM), the homotopy analysis method (HAM), the variational iterative method (VIM), the differential transformation method (DTM), the harmonic balancing method, the Adomian's decomposition method, etc. [11-15] solve nonlinear differential equations without linearization, discretization, or approximation of the derivatives. However, most of the approximate methods give accurate predictions only when the nonlinearities are weak, and they fail to predict accurate solutions for the strong nonlinear models. Also, when these methods are routinely implemented, they can sometimes lead to erroneous results [15]. Additionally, some of them require more mathematical manipulations and are not applicable to all problems, and thus suffer a lack of generality. For example, DTM is proved to be more effective than most of the other approximate analytical solutions as it does not require many computations that are carried out in ADM, HAM, HPM, and VIM. However, the transformation of the nonlinear equations and the development of the equivalent recurrence equations for the nonlinear equations using DTM is proved to be somehow difficult in some nonlinear systems such as the rational Duffing oscillator, the irrational nonlinear Duffing oscillator, and the finite extensibility nonlinear oscillator. Moreover, the determination of the Adomian polynomials as carried out in ADM; the restrictions of HPM to weakly nonlinear problems; the lack of rigorous theories or proper guidance for choosing the initial approximation, the auxiliary linear operators, the auxiliary functions, and the auxiliary parameters in HAM; the operational restrictions to small domains and the search for a particular value for the auxiliary parameter that will satisfy the second boundary condition which leads to additional computational cost in using DTM are the deficiencies of these methods. Therefore, the quest for comparatively simple, flexible, generic, and highly accurate analytical solutions continues. In this work, the variation iteration method (VIM) is used to develop the approximate analytical solutions to the nonlinear vibration analysis of the single-walled carbon nanotube under the slip effects. The variational iteration method is shown to be one of the most effective, accurate, and convenient approximate analytical methods for a large class of weakly and strongly nonlinear equations. It is a user friendly method with reduced size of calculation and direct and straightforward iteration which generates solutions with a rapid rate of convergent without any restrictive assumptions or transformations. In VIM, the initial solution can be freely chosen with some unknown parameters, and the unknown parameters in the initial solution can be achieved easily. Although there is a rigour of step-by-step integrations coupled with the problem of determination of the Lagrange multiplier in the application of VIM with few number of iteration, in some cases, even a single iteration of VIM can converge to correct solutions or results. The analytical solutions which are developed in this work can serve as a starting point for a better understanding of the relationship between the physical quantities of the problems, since they provide continuous physical insights into the problem than the pure numerical or computation methods.

2. Problem formulation based on the nonlocal beam theory

Consider a carbon nanotube (CNT) conveying fluid as shown in Fig.1. Based on the Eringen's nonlocal elasticity theory [16-19], the stress at a reference point x in an elastic continuum depends not only on the strain field at the same point but on the strains at all other points of the body. Therefore, the equation for the linear homogeneous isotropic and the nonlocal elastic solids with zero body force are given as

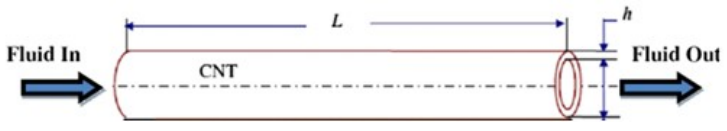

Fig. 1. A carbon nanotube (CNT) conveying fluid

$$\sigma_{ij} = 0 \tag{1}$$

$$\sigma_{ij}(x) = \int_V K\left(|x - x'|, \gamma\right) C_{ijkl}\varepsilon_{kl}(x')dV(x') \tag{2}$$

$$\varepsilon_{ij} = \frac{1}{2}\left(u_{ij} + u_{ji}\right) \tag{3}$$

It can be seen that it is very difficult to solve the elasticity problems by using the integral constitutive relation as given by Eq. (2). Consequently, an alternative and simplified constitutive relation in a differential form is given by Eringen [16-19] as follows:

$$\left(1-\left(e_o a\right)^2 \nabla^2\right)\sigma = T \tag{4}$$

For a nanotube (considering the small-size relation based effect), the nonlocal constitutive relation based on the one-dimension equation of the Eringen's nonlocal theory for the Euler-Bernoulli beam is given as follows:

$$\sigma_{xx} - \left(e_o a\right)^2 \frac{\partial^2 \sigma_{xx}}{\partial x^2} = E\,\varepsilon_{xx} \tag{5}$$

Also, the internal moment for the Euler-Bernoulli beam is given as:

$$T(x,t) = \int_A z\,\sigma_{xx}\,dA \tag{6}$$

where A is the cross sectional area of the nanotube. By substituting σ_{xx} from Eq. (5) into Eq. (6), we have [20]:

$$T(x,t) = \left(e_o a\right)^2 \frac{\partial^2 T}{\partial x^2} - EI\,\frac{\partial^2 w}{\partial x^2} \tag{7}$$

By incorporating the von Karman's nonlinearity, the internal shear force on the structural cross section must satisfy the moment equilibrium relation:

$$Q(x,t) = \frac{\partial T}{\partial x} + N(x,t)\frac{\partial w}{\partial x} \tag{8}$$

It should be pointed out that the internal membrane force N is constant along the beam as:

$$\frac{\partial N}{\partial x} = 0 \quad \Rightarrow N(x,t) = N(t) \tag{9}$$

Therefore, Eq. (9) becomes:

$$Q(x,t) = \frac{\partial T}{\partial x} + N(t)\frac{\partial w}{\partial x} \tag{10}$$

Differentiating Eq. (10) with respect to the spatial variable x considering the absence of an external axial load on the beam yields:

$$\frac{\partial^2 T}{\partial x^2} = \frac{\partial Q}{\partial x} - N(t)\frac{\partial^2 w}{\partial x^2} \tag{11}$$

The differential equation of the motion for the free vibration of the fluid-conveying nanotube can be expressed as:

$$\frac{\partial Q}{\partial x} = m_c \frac{\partial^2 w}{\partial t^2} + F_w \tag{12}$$

where m_c is the mass per unit length of CNT, and F_w is the external force by the fluid on the beam structure which can be expressed as:

$$F_w = m_f \left(2v\,\frac{\partial^2 w}{\partial x\,\partial t} + v^2 \frac{\partial^2 w}{\partial x^2} + \frac{\partial^2 w}{\partial t^2}\right) \tag{13}$$

Therefore,

$$\frac{\partial Q}{\partial x}=m_c\frac{\partial^2 w}{\partial t^2}+m_f\left(2v\frac{\partial^2 w}{\partial x\,\partial t}+v^2\frac{\partial^2 w}{\partial x^2}+\frac{\partial^2 w}{\partial t^2}\right) \tag{14}$$

Substituting Eq. (14) into Eq. (11) gives:

$$\frac{\partial^2 T}{\partial x^2}=m_c\frac{\partial^2 w}{\partial t^2}+m_f\left(2v\frac{\partial^2 w}{\partial x\,\partial t}+v^2\frac{\partial^2 w}{\partial x^2}+\frac{\partial^2 w}{\partial t^2}\right)-N(t)\frac{\partial^2 w}{\partial x^2} \tag{15}$$

For the immovable supports, the internal membrane force is given as:

$$N(t)=\frac{EA}{2L}\int_0^L\left(\frac{\partial w}{\partial x}\right)^2 dx \tag{16}$$

Therefore, eq. (15) can be expressed as:

$$\frac{\partial^2 T}{\partial x^2}=m_c\frac{\partial^2 w}{\partial t^2}+m_f\left(2v\frac{\partial^2 w}{\partial x\,\partial t}+v^2\frac{\partial^2 w}{\partial x^2}+\frac{\partial^2 w}{\partial t^2}\right)-\left[\frac{EA}{2L}\int_0^L\left(\frac{\partial w}{\partial x}\right)^2 dx\right]\frac{\partial^2 w}{\partial x^2} \tag{17}$$

If we substitute Eq. (17) into Eq. (7), we obtaine:

$$T(x,t)=\left(e_o a\right)^2\left[m_c\frac{\partial^2 w}{\partial t^2}+m_f\left(2v\frac{\partial^2 w}{\partial x\,\partial t}+v^2\frac{\partial^2 w}{\partial x^2}+\frac{\partial^2 w}{\partial t^2}\right)-\left[\frac{EA}{2L}\int_0^L\left(\frac{\partial w}{\partial x}\right)^2 dx\right]\frac{\partial^2 w}{\partial x^2}\right]-EI\frac{\partial^2 w}{\partial x^2} \tag{18}$$

Using the Hamilton's principle gives:

$$\begin{aligned}R(x,t)=&\frac{1}{2}\int_0^L m_c\left(\frac{\partial w}{\partial t}\right)^2 dx+\frac{1}{2}\int_0^L\left\{\left(e_o a\right)^2\left[\begin{array}{l}m_c\dfrac{\partial^2 w}{\partial t^2}+m_f\left(2v\dfrac{\partial^2 w}{\partial x\,\partial t}+v^2\dfrac{\partial^2 w}{\partial x^2}+\dfrac{\partial^2 w}{\partial t^2}\right)\\-\left[\dfrac{EA}{2L}\displaystyle\int_0^L\left(\dfrac{\partial w}{\partial x}\right)^2 dx\right]\dfrac{\partial^2 w}{\partial x^2}\end{array}\right]-EI\frac{\partial^2 w}{\partial x^2}\right\}\frac{\partial^2 w}{\partial x^2}dx\\&-\frac{1}{2}\int_0^L\left[\frac{EA}{2L}\int_0^L\left(\frac{\partial w}{\partial x}\right)^2 dx\right]\left(\frac{\partial w}{\partial x}\right)^2 dx\end{aligned} \tag{19}$$

In Eq. (19), the first integral is the kinetic energy of the nanotube, while the second integral represents the elastic energy which is induced by bending, and the third integral is the elastic energy in extension because of the stretching of the neutral axis. From Eq. (19), the nonlinear partial-differential equation of the CNT conveying fluid is expressed as:

$$\begin{aligned}R(x,t)=&EI\frac{\partial^4 w}{\partial x^4}+m\frac{\partial^2 w}{\partial t^2}+2vm_f\frac{\partial^2 w}{\partial x\,\partial t}+m_f v^2\frac{\partial^2 w}{\partial x^2}-\left[\frac{EA}{2L}\int_0^L\left(\frac{\partial w}{\partial x}\right)^2 dx\right]\frac{\partial^2 w}{\partial x^2}\\&-\left(e_o a\right)^2\left[m\frac{\partial^4 w}{\partial x^2\partial t^2}+2vm_f\frac{\partial^4 w}{\partial x^3\partial t}+m_f v^2\frac{\partial^4 w}{\partial x^4}-\left[\frac{EA}{2L}\int_0^L\left(\frac{\partial w}{\partial x}\right)^2 dx\right]\frac{\partial^4 w}{\partial x^4}\right]=0\end{aligned} \tag{20}$$

For the simply supported beam considered in this study, the initial and the boundary conditions are:

$$\begin{aligned}&w(0,x)=A\quad \dot{w}(0,x)=0\\&w(0,t)=w''(0,t)=0\quad w(L,t)=w''(L,t)=0\end{aligned} \tag{21}$$

If the stretching effect in the nanotube is neglected in the Eq. (20), we recovere the classical governing equation for flow-induced vibration of the fluid-conveying nanotube as follows:

$$EI\frac{\partial^4 w}{\partial x^4}+m\frac{\partial^2 w}{\partial t^2}+2vm_f\frac{\partial^2 w}{\partial x\,\partial t}+m_f v^2\frac{\partial^2 w}{\partial x^2}-(e_o a)^2\left[m\frac{\partial^4 w}{\partial x^2\partial t^2}+2vm_f\frac{\partial^4 w}{\partial x^3\partial t}+m_f v^2\frac{\partial^4 w}{\partial x^4}\right]=0 \tag{22}$$

where the natural frequency gives:

$$\omega_n=\left(\frac{n\pi}{L}\right)^2\sqrt{\frac{EI}{m\left\{1+\left((e_o a)\frac{n\pi}{L}\right)^2\right\}}} \tag{23}$$

If the nano-size and the stretching effects are neglected in the Eq. (20), we obtain:

$$EI\frac{\partial^4 w}{\partial x^4}+m\frac{\partial^2 w}{\partial t^2}+2vm_f\frac{\partial^2 w}{\partial x\,\partial t}+m_f v^2\frac{\partial^2 w}{\partial x^2}=0 \tag{24}$$

which is the classical governing equation for the flow-induced vibration of the fluid-conveying pipe, where the natural frequency gives:

$$\omega_n=\left(\frac{n\pi}{L}\right)^2\sqrt{\frac{EI}{m}} \tag{25}$$

For CBT conveying fluid, the radius of the tube is assumed to be the characteristics length scale, the Knudsen number is larger than 10^{-2}. Therefore, the assumption of the no-slip boundary conditions does not hold, and the modified model should be used as follows:

$$VCF=\frac{U_{avg,slip}}{U_{avg,no-slip}}=(1+a_k Kn)\left[4\left(\frac{2-\sigma_v}{\sigma_v}\right)\left(\frac{Kn}{1+Kn}\right)+1\right] \tag{26}$$

where Kn is the Knudsen number, and σ_v is the tangential moment accommodation coefficient which is considered to be 0.7 for most practical purposes [21].

$$a_k=a_o\frac{2}{\pi}\left[tan^{-1}\left(a_1 Kn^B\right)\right] \tag{27}$$

$$a_o=\frac{64}{3\pi\left(1-\frac{4}{b}\right)} \tag{28}$$

Therefore,

$$U_{avg,slip}=(1+a_k Kn)\left[4\left(\frac{2-\sigma_v}{\sigma_v}\right)\left(\frac{Kn}{1+Kn}\right)+1\right]U_{avg,no-slip}=VCF\left(U_{avg,no-slip}\right) \tag{29}$$

and Eq. (20) could be written as:

$$\begin{aligned}R(x,t)=&EI\frac{\partial^4 w}{\partial x^4}+m\frac{\partial^2 w}{\partial t^2}+2m_f\left[VCF\left(U_{avg,no-slip}\right)\right]\frac{\partial^2 w}{\partial x\,\partial t}\\&+m_f\left[VCF\left(U_{avg,no-slip}\right)\right]^2\frac{\partial^2 w}{\partial x^2}-\left[\frac{EA}{2L}\int_0^L\left(\frac{\partial w}{\partial x}\right)^2 dx\right]\frac{\partial^2 w}{\partial x^2}\\&-(e_o a)^2\left[\begin{array}{l}m\dfrac{\partial^4 w}{\partial x^2\partial t^2}+2m_f\left[VCF\left(U_{avg,no-slip}\right)\right]\dfrac{\partial^4 w}{\partial x^3\partial t}\\+m_f\left[VCF\left(U_{avg,no-slip}\right)\right]^2\dfrac{\partial^4 w}{\partial x^4}-\left[\dfrac{EA}{2L}\displaystyle\int_0^L\left(\dfrac{\partial w}{\partial x}\right)^2 dx\right]\dfrac{\partial^4 w}{\partial x^4}\end{array}\right]=0\end{aligned} \tag{30}$$

Using the Galerkin's decomposition procedure to separate the spatial and temporal parts of the lateral displacement functions as:

$$w(x,t)=\phi(x)u(t) \tag{31}$$

where $u(t)$ is the generalized coordinate of the system, and $\phi(x)$ is a trial or comparison function that will satisfy both the geometric and the natural boundary conditions.

Applying the one-parameter Galerkin's solution given in Eq. (31) to Eq. (30) yields:

$$\int_0^L R(x,t)\phi(x)dx \tag{32}$$

where

$$\begin{aligned} R(x,t) &= EI\frac{\partial^4 w}{\partial x^4}+m\frac{\partial^2 w}{\partial t^2}+2m_f\left[VCF\left(U_{avg,no-slip}\right)\right]\frac{\partial^2 w}{\partial x\,\partial t} \\ &+m_f\left[VCF\left(U_{avg,no-slip}\right)\right]^2\frac{\partial^2 w}{\partial x^2}-\left[\frac{EA}{2L}\int_0^L\left(\frac{\partial w}{\partial x}\right)^2 dx\right]\frac{\partial^2 w}{\partial x^2} \\ &-(e_o a)^2\left[\begin{array}{l} m\dfrac{\partial^4 w}{\partial x^2\partial t^2}+2m_f\left[VCF\left(U_{avg,no-slip}\right)\right]\dfrac{\partial^4 w}{\partial x^3\partial t} \\ +m_f\left[VCF\left(U_{avg,no-slip}\right)\right]^2\dfrac{\partial^4 w}{\partial x^4}-\left[\dfrac{EA}{2L}\displaystyle\int_0^L\left(\dfrac{\partial w}{\partial x}\right)^2 dx\right]\dfrac{\partial^4 w}{\partial x^4} \end{array}\right]=0 \end{aligned} \tag{33}$$

For the simply-supported nanotube

$$\phi(x)=\sin\beta_n x \tag{34}$$

where

$$\sin\beta_n L=0 \quad\Rightarrow \beta_n=\frac{n\pi}{L} \quad n=1,\ 2,\ 3,\ 4....$$

we arrived at

$$M\ddot{u}_s(t)+G\dot{u}_s(t)+(K+C)u_s(t)-Vu_s^3(t)=0 \tag{35}$$

where

$$u_s=VCF\left(U_{avg,no-slip}\right)$$

$$M=\int_0^L(m_p+m_f)\phi(x)\left(\phi(x)-(e_o a)^2\frac{d^2\phi}{dx^2}\right)dx$$

$$G=\int_0^L\phi(x)\left\{2m_f u_s\left(\frac{d\phi}{dx}-(e_o a)^2\frac{d^3\phi}{dx^3}\right)\right\}dx$$

$$K=\int_0^L EI\,\phi(x)\frac{d^4\phi}{dx^4}dx$$

$$C=\int_0^L m_f u_s^2\phi(x)\left(\frac{d^2\phi}{dx^2}-(e_o a)^2\frac{d^4\phi}{dx^4}\right)dx$$

$$V=\int_0^L\frac{EA}{2L}\phi(x)\left\{\left[\int_0^L\left(\frac{\partial\phi}{\partial x}\right)^2 dx\right]-\left\{\frac{d^2\phi}{dx^2}-(e_o a)^2\frac{d^4\phi}{dx^4}\right\}\right\}dx$$

Under the transformation, $\tau=\omega t$, Eq. (35) turns out to be:

$$M\omega^2\ddot{u}(\tau)+G\omega\dot{u}(\tau)+(K+C)u(\tau)-Vu^3(\tau)=0 \tag{36a}$$

For the undamped simple-simple supported structures $G = 0$ we have:

$$M\omega^2\ddot{u}(\tau)+(K+C)u(\tau)-Vu^3(\tau)=0 \tag{36b}$$

3. Method of solution: Variational iteration method

It is very difficult to generate any closed form solution for the above nonlinear simultaneous Eqs. (36a) and (36b). However, a closed form series solution or an approximate analytical solution can be obtained for the non-linear differential equations. In finding direct and practical solutions to the problem, the variational iteration method is applied to the nonlinear equations. As pointed previously, the variational iteration method is an approximate analytical method for solving the differential equations. The basic definitions of the method are as follows:

The differential equation to be solved can be written in the following form:

$$Lu+Nu=g(t) \tag{37}$$

Where L is a linear operator, N is a nonlinear operator, and $g(t)$ is an inhomogeneous term in the differential equation.

Following the VIM procedure, we have a correction functional stationary as:

$$u_{n+1}(t)=u_n(t)+\int_0^t\lambda\left\{Lu_n(\tau)+N\tilde{u}(\tau)-g(t)\right\}d\tau \tag{38}$$

where λ is a general Lagrange multiplier, the subscript n is the nth approximation, and $\tilde{u}$ is a restricted variation $\delta\tilde{u}=0$. Making the above correction functional stationary and considering $\delta u_{n+1}=0$, we have:

$$\delta u_{n+1}(t)=\delta u_n(t)+\lambda(\delta u_n)'\Big|_0^t-\lambda'(\delta u_n)\Big|_0^t+\int_0^t\left\{\lambda''+\lambda\left(\frac{K+C}{M}\right)\right\}\delta u_n d\tau=0 \tag{39}$$

where its stationary conditions are as follows:

$$\begin{aligned}&1-\lambda'(\tau)\big|_{\tau=t}=0\\&\lambda(\tau)\big|_{\tau=t}=0\\&\lambda''(\tau)+\left(\frac{K+C}{M}\right)\lambda(\tau)=0\end{aligned} \tag{40}$$

By solving Eq. (40), we have a Lagrange multiplier as:

$$\lambda(\tau)=\sqrt{\frac{M}{K+C}}\int_0^t sin\left\{\sqrt{\frac{K+C}{M}}(\tau-t)\right\} \tag{41}$$

therefore, Eq. (38) can be written as:

$$u_{n+1}=u_n+\sqrt{\frac{M}{K+C}}\int_0^t sin\left\{\sqrt{\frac{K+C}{M}}(\tau-t)\right\}\left\{M\omega^2\frac{d^2u_n}{d\tau^2}+(K+C)u_n-Vu_n^3\right\}d\tau \tag{42}$$

In order to find the periodic solution of Eq. (42), assume an initial approximation for the zero-order deformation to be as:

$$u_o(\tau)=A\cos\tau \tag{43}$$

Then, the residual is given as:

$$R(\tau) = -M\,\omega_o^2 A\cos\tau + (K+C)A\cos\tau - VA^3\cos^3\tau \tag{44}$$

which is also given as:

$$R(\tau) = -M\,\omega^2 A\cos\tau + (K+C)A\cos\tau - VA^3\left(\frac{3\cos\tau+\cos 3\tau}{4}\right) \tag{45}$$

Collecting like terms at RHS gives:

$$R(\tau) = \left((K+C)A - \frac{3VA^3}{4} - M\,\omega^2 A\right)\cos\tau - \frac{1}{4}VA^3\cos 3\tau \tag{46}$$

In order to eliminate the secular term, the coefficient of $\cos\tau$ must be vanished. Therefore,

$$\left((K+C)A - \frac{3VA^3}{4} - M\,\omega_o^2 A\right) = 0 \tag{47}$$

Thus, for the zero-order nonlinear natural frequency, we have:

$$\omega_o \approx \sqrt{\frac{K+C}{M} - \frac{3VA^2}{4M}} \tag{48}$$

Therefore, the ratio of the zero-order nonlinear natural frequency ω_o to the linear frequency ω_b yields:

$$\frac{\omega_o}{\omega_b} \approx \sqrt{1 - \frac{3VA^2}{4(K+C)}} \tag{49}$$

where

$$\omega_b = \sqrt{\frac{K+C}{M}}$$

Similarly, for the first-order nonlinear natural frequency, we have:

$$\omega_1 \approx \sqrt{\frac{1}{2}\left\{\left[\left(\frac{K+C}{M}\right) - \left(\frac{3VA^2}{4M}\right)\right] + \sqrt{\left[\left(\frac{K+C}{M}\right) - \left(\frac{3VA^2}{4M}\right)\right]^2 - \left(\frac{3V^2A^4}{32M^2}\right)}\right\}} \tag{50}$$

The ratio of the first-order nonlinear frequency ω_1 to the linear frequency ω_b will be:

$$\frac{\omega_1}{\omega_b} \approx \sqrt{\frac{1}{2}\left\{\left[1 - \left(\frac{3VA^2}{4(K+C)}\right)\right] + \sqrt{\left[1 - \left(\frac{3VA^2}{4(K+C)}\right)\right]^2 - \left(\frac{3V^2A^4}{32(K+C)}\right)}\right\}} \tag{51}$$

For the first iteration,

$$u_1 = u_0 + \int_0^t \lambda(\tau)R_0(\tau)\,d\tau \tag{52}$$

By substituting Eqs. (41), (43), and (46) into Eq. (52), we have:

$$u_1 = u_0 + \sqrt{\frac{M}{K+C}}\int_0^t \sin\left\{\sqrt{\frac{K+C}{M}}(\tau - t)\right\}\left\{M\,\omega^2\ddot{u}_0 + (K+C)u_0 - Vu_0^3\right\}d\tau \tag{53}$$

By substituting Eq. (43) into Eq. (53), we have:

$$u_1 = A\cos\tau + \sqrt{\frac{M}{K+C}}\int_0^t \sin\left\{\sqrt{\frac{K+C}{M}}(\tau - t)\right\}\left\{-M\omega_o^2 A\cos\tau + (K+C)A\cos\tau - VA^3\cos^3\tau\right\}d\tau \tag{54}$$

A further simplification gives:

$$u_1 = \frac{K+C}{9M\omega^2 - K + C}\left\{\frac{9AM\omega^2}{K+C}\cos\tau - A\cos\tau - \frac{A^3}{16}\cos\tau + \frac{A^3}{16}\cos(3\tau)\right\} \tag{55}$$

which can be written as:

$$u(t) \approx \left(\frac{K+C}{9M\omega^2 - K + C}\right)\left\{\frac{9AM\omega^2}{K+C}\cos(\omega t) - A\cos(\omega t) - \frac{A^3}{16}\cos(\omega t) + \frac{A^3}{16}\cos(3\omega t)\right\} \tag{56}$$

Substituting Eqs. (34) and (56) into Eq. (32), we have:

$$w(x,t) \approx \left(\frac{K+C}{9M\omega^2 - K + C}\right)\left\{\frac{9AM\omega^2}{K+C}\cos(\omega t) - A\cos(\omega t) - \frac{A^3}{16}\cos(\omega t) + \frac{A^3}{16}\cos(3\omega t)\right\}\sin\frac{n\pi x}{L} \tag{57}$$

where

$$\omega \approx \sqrt{\frac{1}{2}\left\{\left[\left(\frac{K+C}{M}\right) - \left(\frac{3VA^2}{4M}\right)\right] + \sqrt{\left[\left(\frac{K+C}{M}\right) - \left(\frac{3VA^2}{4M}\right)\right]^2 - \left(\frac{3V^2A^4}{32M^2}\right)}\right\}}$$

It can easily be seen that as the nonlinear term tends to zero, the frequency ratio of the nonlinear frequency to the linear frequency ω/ω_b tends to 1.

$$\lim_{\xi_2 \to 0}\frac{\omega}{\omega_b} = 1 \tag{58}$$

Also, as the amplitude A tends to zero, the frequency ratio of the nonlinear frequency to the linear frequency ω/ω_b tends to 1.

$$\lim_{A \to 0}\frac{\omega}{\omega_b} = 1 \tag{59}$$

For very large values of the amplitude A, we have:

$$\lim_{A \to \infty}\frac{\omega}{\omega_b} = \infty \tag{60}$$

4. Results and Discussion

The first five normalized mode shapes of the beams simple-simple are shown in Fig. 2. Moreover, the figure shows the deflections of the beam along the beams' span at five different buckled and mode shapes.

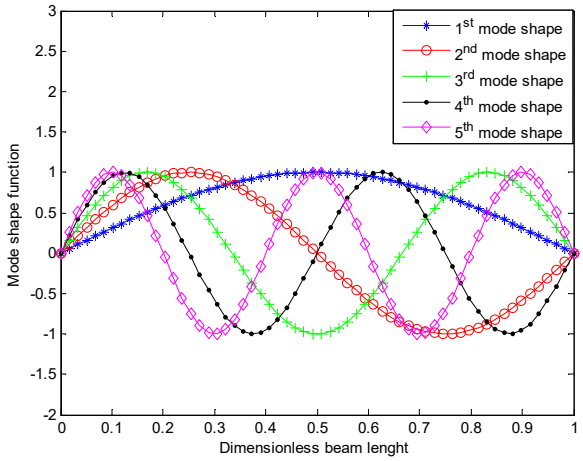

Fig. 2. The first five normalized mode shaped of the under simple supports nanotube

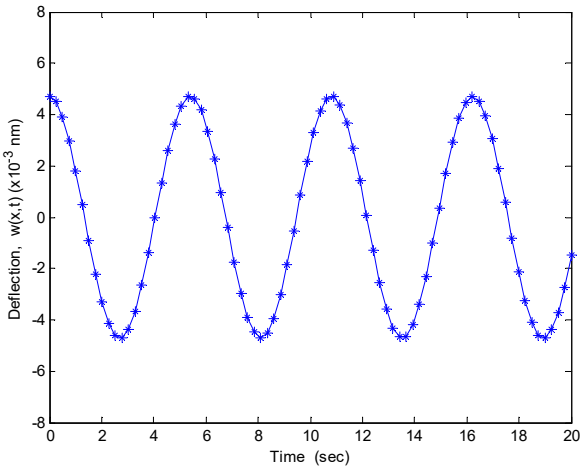

Fig. 3. Midpoint deflection time history for the nonlinear analysis of SWCBT when Kn=0.03 and U= 100 m/s

The effects of the slip parameter called the Knudsen number and the fluid flow velocity on the deflection of the nanotube are presented in Figs. 3-5. Fig. 3 illustrates the midpoint deflection time history for the nonlinear analysis of SWCBT when *Kn = 0.03* and *U= 100 m/s*, while Fig. 4 presents the midpoint deflection time history for the nonlinear analysis of SWCBT when *Kn = 0.03* and *U= 500 m/s*. Furthermore, Fig. 5 depicts the midpoint deflection time history for the nonlinear analysis of SWCBT when *Kn = 0.1* and *U= 500 m/s*, while Fig. 6 shows the midpoint deflection time history when *Kn = 0.05*, *U= 500 m/s*, and when *Kn = 0.1* and *U= 500 m/s,* respectively. Fig. 7 shows the comparison of the linear vibration with the nonlinear vibration of SWCNT. It could be seen in the figure that the discrepancy between the linear and nonlinear amplitudes increases with increment of the maximum vibration. These results are in line with the results obtained by Ali-Asgari *et al.* [20].

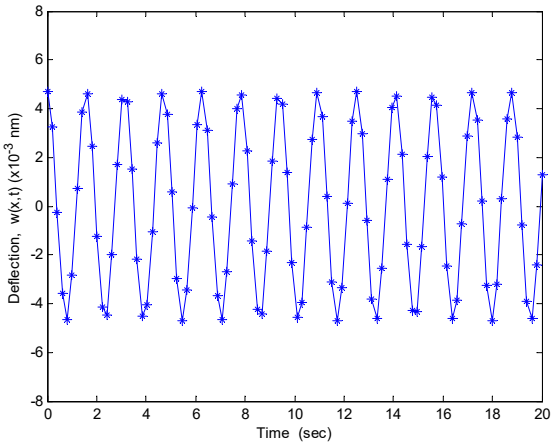

Fig. 4. Midpoint deflection time history for the nonlinear analysis of SWCBT when Kn=0.03 and U= 500 m/s

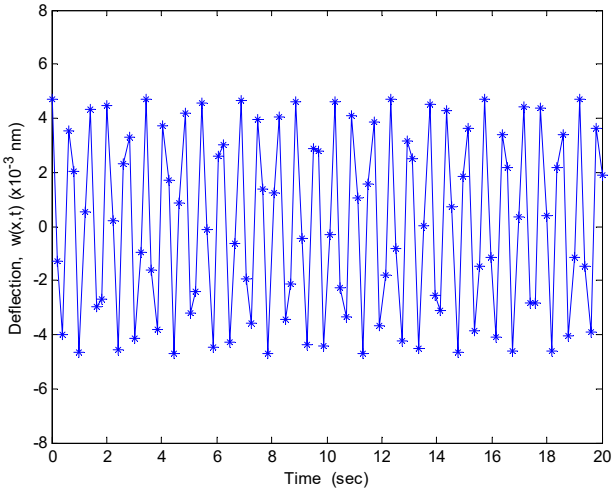

Fig. 6. Midpoint deflection time history for the linear analysis of SWCBT when Kn=0.1 and U= 500 m/s

The effects of the slip parameter, the Knudsen number, on the dimensionless frequency ratio of the nanotube are shown in Figs. 8. It is depicted that an increase in the slip parameter leads to a decrease in the dimensionless

frequency ratio of the vibration of SWCNT. It should be pointed out that the Knudsen number predicts various flow regimes in the fluid-conveying nanotube. The Knudsen number with zero value has the highest frequency as shown in the figure. As the Knudsen number increases, the bending stiffness of the nanotube decreases; as a consequent, the critical continuum flow velocity decreases as the curves shift to the lowest frequency zone.

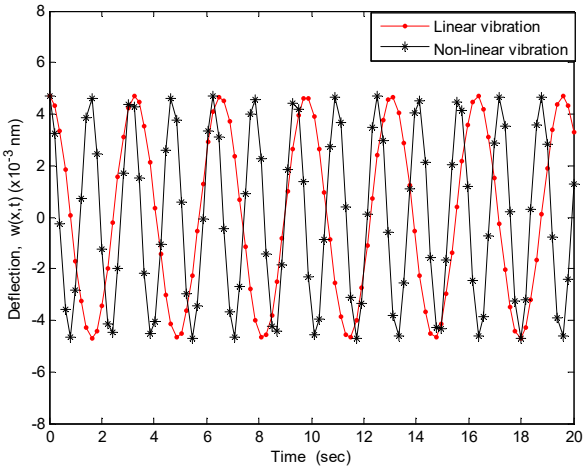

Fig. 7. Comparison of the midpoint deflection time history for the linear and nonlinear analysis of CBT when Kn=0.03 and U= 500 m/s

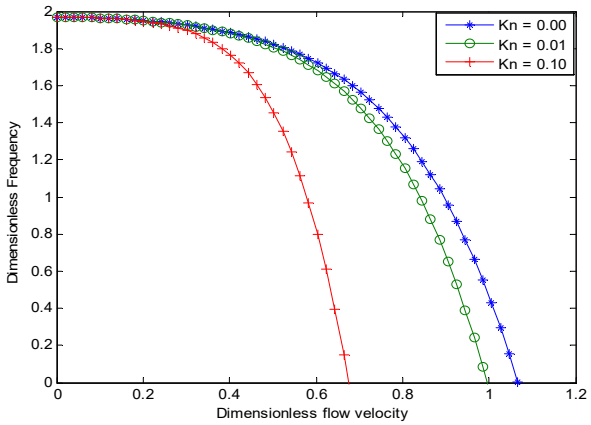

Fig. 8. Effects of the Knudsen number on the dimensionless frequency of the simply supported single-walled nanotube

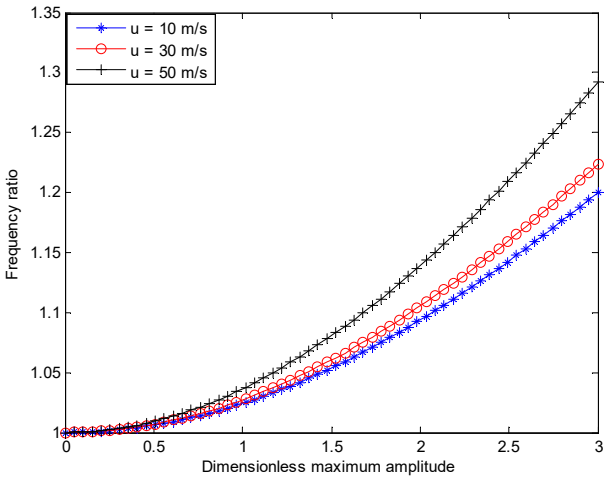

Fig. 9. Effects of the fluid-flow velocity on the nonlinear amplitude-frequency response curves of the nanotube

Fig. 9 shows the effects of the fluid-flow velocity on the nonlinear amplitude-frequency response curves of the nanotube. It is observed that as the fluid-flow velocity increases, the nonlinear vibration frequency ratio increases, and the difference between the nonlinear and linear frequency becomes pronounced. The results in Fig. 9 reveal that the fluid flow velocity has significant effects on the nonlinear behaviour of the nanotube, therefore, this and other significant parameters can be used to control the nonlinearity of the structure.

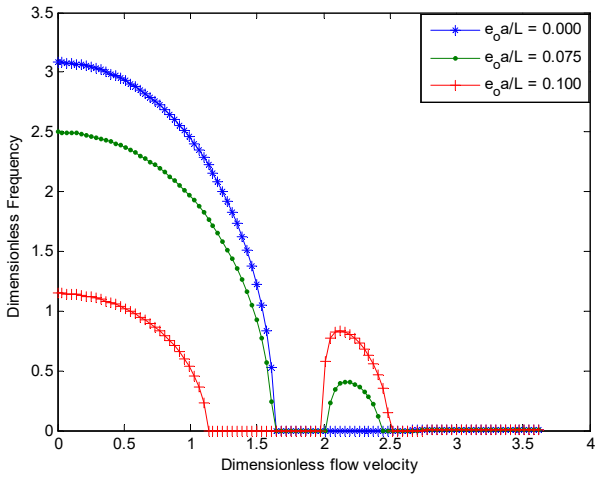

Fig. 10. Effects of the nonlocal parameter on the natural frequency of the nonlinear vibration

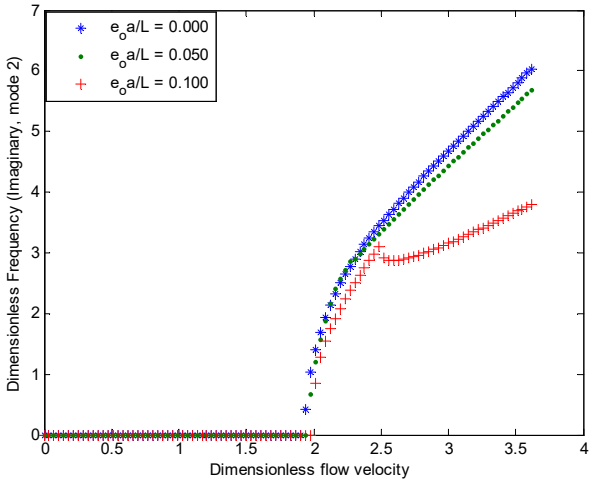

Fig. 11. Effects of the nonlocal parameter on the natural frequency of the nonlinear vibration

The studies and the investigations of the dynamic and stability behaviours of the structure are largely dependent on the effects of the fluid flow velocity and amplitude on the natural frequencies of the vibration. The effects of the nonlocal parameter on the vibration of the nanotube are shown in Figs. 10-11. It is depicted that an increase in the slip parameter leads to a decrease in the frequency of the vibration of the structure and the critical velocity of the conveyed fluid. It should be pointed out, as shown in the figures, that the zero value for the nonlocal parameter, i.e., $e_o a = 0$, represents the results of the classical Euler-Bernoulli model which has the highest frequency and critical fluid velocity (a point where the structure starts to experience instability). When the flow velocity of the fluid attains the critical velocity, both the real and imaginary parts of the frequency are equal to zero. Additionally, the figures present the critical speeds corresponding to the divergence conditions for different values of the nonlocal parameters. In Figs. 10 and 11, the real and imaginary parts of the eigenvalues related to the two lowest modes with different nanotube parameters are shown.

7. Conclusion

In this work, the analytical solutions have been provided to analyze the effects of the slip boundary conditions on the nonlinear dynamic behaviours of the carbon nanotube conveying fluid using the variation iteration method. The results show that the alteration of the nonlinear flow-induced frequency from the linear frequency is significant as the amplitude, the flow velocity, and the aspect ratio increase. The analytical solutions can serve as benchmarks for other methods of the solutions of the problem. They can also provide a starting point for a better understanding of the relationship between the physical quantities of the problems.

Nomenclature

A	Area of the structure
E	Young Modulus of Elasticity
I	moment of area
Kn	Knudsen number

l_o, l_1, l_2	independent length scale parameters
L	length
m_p	mass of the structure
m_f	mass of fluid
N	axial/Longitudinal force
r	radius of the structure
t	time
$u(t)$	generalized coordinate of the system
w	transverse displacement/deflection
x	axial coordinate
$Z_o(x)$	the arbitrary initial rise function
σ_v	tangential moment accommodation coefficient
$\phi(x)$	trial/comparison function
υ	Poisson' ratio
μ	damping coefficient

References

1. Iijima, S. Helical microtubules of graphitic carbon. Nature, London, Vol. 354, no. 6348, pp. 56–58, 1991.
2. Yoon, G., Ru, C.Q., Mioduchowski, A. Vibration and instability of carbon nanotubes conveying fluid. Journal of Applied Mechanics, Transactions of the ASME, Vol. 65, no. 9, 1326–1336, 2005.
3. Yan, Y., Wang, W.Q. and Zhang, L.X. Nonlocal effect on axially compressed buckling of triple-walled carbon nanotubes under temperature field. Journal of Applied Math and Modelling, Vol. 34, pp. 3422–3429, 2010.
4. Murmu, T., and Pradhan, S. C. Thermo-mechanical vibration of Single-walled carbon nanotube embedded in an elastic medium based on nonlocal elasticity theory. Computational Material Science, Vol. 46, pp. 854–859, 2009.
5. Yang, H. K. and Wang, X. Bending stability of multi-wall carbon nanotubes embedded in an elastic medium. Modeling and Simulation in Materials Sciences and Engineering, Vol. 14, pp. 99–116, 2006.
6. Yoon, J. Ru, C.Q., Mioduchowski, A. Vibration of an embedded multiwall carbon nanotube. Composites Science and Technology, Vol. 63, no. 11, pp. 1533–1542, 2003.
7. Lu, P. Lee, H.P., Lu, C. Zhang, P.Q. Application of nonlocal beam models for carbon nanotubes. International Journal of Solids and Structures, Vol. 44, no. 16, pp. 5289–5300, 2007.
8. Zhang, Y., Liu, G., Han, X. Transverse vibration of double-walled carbon nanotubes under compressive axial load. Applied Physics Letter A, Vol. 340, no. 1-4, pp. 258–266, 2005.
9. GhorbanpourArani, M.S. Zarei, M. Mohammadimehr, A. Arefmanesh, M.R. Mozdianfard. The thermal effect on buckling analysis of a DWCNT embedded on the Pasternak foundation", Physica E, Vol. 43, pp. 1642–1648, 2011.
10. Sobamowo, M. G. Thermal analysis of longitudinal fin with temperature-dependent properties and internal heat generation using Galerkin's method of weighted residual. Applied Thermal Engineering Vol. 99, pp.1316–1330, 2016.
11. Rafei, M. Ganji, D. D. Daniali, H., Pashaei. H. The variational iteration method for nonlinear oscillators with discontinuities. J. Sound Vib. Vol. 305, pp. 614–620, 2007.
12. S. S. Ganji, D. D. Ganji, D. D., H. Ganji, Babazadeh, Karimpour, S.: Variational approach method for nonlinear oscillations of the motion of a rigid rod rocking back and cubic-quintic duffing oscillators. Prog. Electromagn. Res. M Vol. 4, pp. 23–32, 2008.
13. Liao, S. J. The Proposed Homotopy Analysis Technique for the Solution of Nonlinear Problems,Ph. D. dissertation, Shanghai Jiao Tong University, 1992
14. Zhou, J. K. Differential Transformation and its Applications for Electrical Circuits. *Huazhong University Press: Wuhan, China,* 1986.
15. Fernandez, A. On some approximate methods for nonlinear models. Appl Math Comput., Vol. 21., pp. 168-74, 2009
16. Eringen, A. C. "On differential equations of nonlocal elasticity and solutions of screw dislocation and surface waves", Journal of Applied Physics, Vol. 54, no. 9, pp.4703–4710, 1983.
17. Eringen, A. C. "Linear theory of nonlocal elasticity and dispersion of plane waves", Inter- national Journal of Engineering Science, Vol. 10, no. (5), pp. 425–435, 1972.
18. Eringen, A. C. and Edelen, D. G., B. "On nonlocal elasticity", International Journal of Engineering Science, Vol. 10(3), pp. 233–248, 1972.
19. Eringen, A. C. "Nonlocal continuum field theories", Springer, New York 2002.

20. Ali-Asgari, M., Mirdamadi, H. R. and Ghayour, M. Coupled effects of nano-size, stretching, and slip boundary conditions on nonlinear vibrations of nano-tube conveying fluid by the homotopy analysis method.Physica E, Vol. 52, pp. 77–85, 2013.
21. Shokouhmand, H. Isfahani, A. H. M. and Shirani, E. “Friction and heat transfer coefficient in micro and nano channels with porous media for wide range of Knudsen number”, International Communication in Heat and Mass Transfer, Vol. 37, pp. 890-894, 2010.